A Holographic Projection System With an Electrically Adjustable Optical Zoom and a Fixed Location of Zeroth-Order Diffraction

Ming-Syuan Chen, Neil Collings, Hung-Chun Lin, and Yi-Hsin Lin

***Abstract*—An electrically tunable optical zooming holographic projection system with a fixed location of zeroth-order diffraction is demonstrated. By using two liquid lenses and an encoded Fresnel lens on a liquid crystal on silicon (LCoS) panel, the size of the projected image of the holographic projection system is changeable; meanwhile, the locations of both of the zeroth-order diffraction and the first-order diffraction are unchanged. Therefore, the zeroth-order diffraction can be removed by using a fixed optical high-pass filter. We can use it to realize an image size matching system for green light (532 nm) and red light (632.8 nm) without any positional motion of the optical elements. The optical zoom function enhances the feasibility to realize a high-resolution full-color holographic projection system.**

***Index Terms*—Holographic projection, liquid lens.**

I. Introduction

MICRODISPLAYS are commonly used in two types of projection systems, one is a conventional projection system based on amplitude modulations of microdisplays, the other is a holographic projection system based on phase or amplitude modulations of microdisplays to generate the diffraction patterns [1]–[3]. The advantages of holographic projections are high light efficiency and the feasibility of real 3D images [4]. Nevertheless, the different wavelengths of coherent light sources result in a mismatch of chromatic image sizes for full color applications [5]–[7]. To solve the mismatch of chromatic images, we proposed a holographic projection system adopting a liquid crystal lens to optically adjust the chromatic image sizes [8]. Makowski *et al.* proposed a method to divide the liquid crystal on silicon (LCoS) panel into three subzones for different computer generated holograms (CGH) [9]. However, many problems still need to be overcome, such as the slow response time of the liquid crystal lens (>2 seconds), the reduction of the resolution of the image due to subzones, and vignetting resulting from the small aperture size ($\sim$ 2 mm). Moreover, the location of the projected image of the zeroth-order diffraction varies when we adjust the size of the projected image at different wavelengths. In order to eliminate the zeroth-order diffraction, we can mechanically adjust the location of an optical high pass filter and the system is then bulky for practical applications. In this paper, we demonstrate a holographic projection system using two liquid lenses which exhibits not only an electrically tunable optical zoom, but also a fixed location of projected image of zeroth-order diffraction. The aperture size of the liquid lens is large ($\sim$ 1 cm) and the switching time is fast (<80 ms). We can eliminate the zeroth-order diffraction without mechanically changing the position of the optical high pass filter. In addition, the zoom ratio of the first-order diffraction is 1.98:1. The system we propose is more practical for full color holographic projections based on the time-sequential projection approach, i.e., a single-panel solution. A single-panel solution allows a simpler optical system and a reduced cost compared with a three-panel solution. Moreover, our proposed system not only solves the mismatch of the chromatic image size, but also the positional shift of the zeroth-order diffraction.

II. Structure and Operating Principle

The holographic projection system with an electrically tunable optical zoom consists of lasers, two beam expanders, a beam splitter, a polarizer, an analyzer, a mirror, reflective liquid crystal on silicon (LCoS) panel, one solid lens, two liquid lenses, an optical high-pass filter and a screen for observation, as shown in Fig. 1(a). The lasers we used were a He–Ne Laser ($\lambda = 632.8$ nm) and a diode pumped solid state laser ($\lambda = 532$ nm). The transmission axes of polarizer and analyzer are parallel to each other. The angle between the direction of linearly polarized light and the x-axis of LCoS panel is 45 degree.

The phase information created by the phase modulation of the LCoS panel includes a Fourier hologram and an encoded Fresnel lens. The function of "liquid lens 1" is to control the divergence of the laser beams impinging on the LCoS panel [equivalent to adjusting d_1 in Fig. 1(b)]. Two electrically tuning lenses: the Fresnel lens encoded on the LCoS panel and the "liquid lens 2", are optical elements in charge of the function of optical zoom to adjust the image sizes at different wavelengths (chromatic image size). The "solid lens" is used to observe the Fourier transform of the hologram displayed on the LCoS panel, in the effective back focal plane of the "solid lens". The high

Manuscript received October 29, 2013; revised December 26, 2013; accepted January 23, 2014. Date of publication January 28, 2014; date of current version May 05, 2014. This work was supported by the National Science Council (NSC) in Taiwan under Contract 101-2112-M-009-011-MY3. The work of N. Collings was supported by the EPSRC through *Liquid Crystal Photonics* Platform Grant EP/F00897X/1.

M.-S. Chen, H.-C. Lin, and Y.-H. Lin are with the Department of Photonics, National Chiao Tung University, Hsinchu 30010, Taiwan.

N. Collings is with the Engineering Department, Cambridge University, Cambridge CB3 0FA, U.K. (e-mail: nc229@cam.ac.uk).

Color versions of one or more of the figures are available online at http://ieeexplore.ieee.org.

Digital Object Identifier 10.1109/JDT.2014.2303132

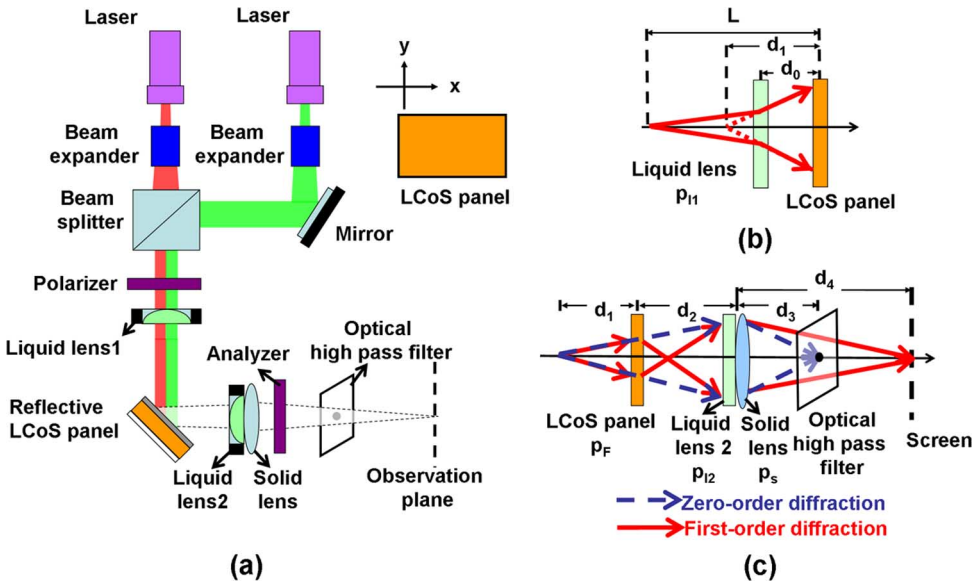

Fig. 1. (a) Structure of the image matching holographic projection system. (b) Schematic illustration of the liquid lens 1 and LCoS panel in (a). (c) Schematic effective optical system of (a) with zeroth-order diffraction and first-order diffraction.

pass filter is a transparency with a black area to block the beam spot of zeroth-order diffraction.

Fig. 1(b) is the schematic effective optical system of the liquid lens 1 and LCoS panel in Fig. 1(a). L is the distance between laser and LCoS panel, d_0 is the distance between the "liquid lens 1" and LCoS panel, and d_1 is the distance between the image plane of the "liquid lens 1" and LCoS panel. Assume the lens power of the "liquid lens 1" is p_{l1}. According to the thin lens formula, d_1 can be expressed as a function of p_{l1}:

$$d_1(p_{l1}(\lambda)) = \frac{p_{l1}(\lambda)\cdot d_0\cdot(d_0-L)+L}{p_{l1}(\lambda)\cdot(d_0-L)+1}, \tag{1}$$

where λ is the wavelength. The effective optical system is depicted in Fig. 1(c), where the light source is a spherical wave originating at a distance d_1 in front of the LCoS panel. d_1 can be controlled electrically by the "liquid lens 1". The distance between the LCoS panel and "liquid lens 2" is d_2, d_3 is the distance between the solid lens and the image of the zeroth-order diffraction, and d_4 is the distance between the solid lens and the image of the first-order diffraction. We place an optical high pass filter to filter out zeroth-order diffraction and a screen for observation of the image of the first-order diffraction. Assume p_F, p_{l2}, and p_s are the lens powers of the encoded Fresnel lens, "liquid lens 2", and "solid lens", respectively. The "liquid lens 2" and "solid lens" are attached together and the effective lens power (p_{ls}) of the combination then equals the summation of the two lens powers (i.e., $\mathrm{p}_{ls} = \mathrm{p}_{l2} + \mathrm{p}_s$). The lens power of the encoded Fresnel lens does not affect the location of the zeroth-order diffraction. According to the thin lens formula, d_3 can be expressed as

$$d_3(p_{ls}(A,\lambda),d_1(\mathrm{p}_{l1}(\lambda))) = \frac{d_1(\mathrm{p}_{l1}(\lambda))+d_2}{p_{ls}(A,\lambda)\times[d_1(\mathrm{p}_{l1}(\lambda))+d_2]-1} \tag{2}$$

where A is the electric current of the "liquid lens 2". In (2), d_2 is a constant and d_3 is a function of p_{ls} and d_1. Equation (2) indicates that the image of zeroth-order diffraction changes with the lens powers of the "liquid lens 1"and the "liquid lens 2". For practical applications, the image of the zeroth-order diffraction should be fixed (i.e., $\mathrm{d}_3 = \text{constant} \equiv c_1$); otherwise, the high pass filter has to be moved accordingly to filter out the zeroth-order diffraction. We actually can adjust d_1 and p_{ls} to fix the image location of the zeroth-order diffraction. d_1 and p_{ls} have to satisfy (3) which is derived by rearranging (2)

$$\mathrm{d}_1(\mathrm{p}_{l1}(\lambda)) = \frac{d_2\cdot \mathrm{c}_1\cdot p_{ls}(A,\lambda)-\mathrm{d}_2-c_1}{1-\mathrm{c}_1\cdot p_{ls}(A,\lambda)}. \tag{3}$$

Next, we use the Nazarathy and Shamir operator method to analyze the first-order diffraction in a coherent optical system [10], [11]. The transform operator T of the optical system can be expressed as

$$\begin{aligned} T =& R[d_4]\cdot Q[-p_{ls}(\mathrm{A},\lambda)]\cdot R[d_2]\cdot f(x,y)\cdot Q[-p_F(\lambda)] \\ &\cdot Q\left[\frac{1}{d_1(p_{l1}(\lambda))}\right] \end{aligned} \tag{4}$$

where $f(x,y)$ and p_F are the Fourier hologram and the lens power of the encoded Fresnel lens displayed on the LCoS panel, respectively. Q is the operator for the multiplication by a quadratic-phase exponential. R is the operator for free-space propagation. The lens power of the encoded Fresnel lens $p_F(\lambda)$ is adjustable by setting the phase profile of the encoded Fresnel lens. According to the relations between the operators, (4) can be rewritten as

$$\begin{aligned} T = Q&\left[\frac{p_{ls}(A,\lambda)}{d_4\cdot p_{ls}-1}+\left(\frac{1}{1-d_4\cdot p_{ls}(A,\lambda)}\right)^2\cdot\frac{1}{d_2+\frac{d_4}{1-d_4\cdot p_{ls}(A,\lambda)}}\right] \\ &\cdot V\left[\frac{1}{1-d_4\cdot p_{ls}(A,\lambda)}\cdot\frac{1}{\lambda\left(d_2+\frac{d_4}{1-d_4\cdot p_{ls}(A,\lambda)}\right)}\right]\cdot Ff \\ &\cdot Q\left[\frac{1}{d_2+\frac{d_4}{1-d_4\cdot p_{ls}(A,\lambda)}}-p_F(\lambda)+\frac{1}{d_1(p_{l1}(\lambda))}\right]. \end{aligned} \tag{5}$$

In (5), the operator, F, is the Fourier transform, and the operator, V, is scaling by a constant. The first Q operator in (5) can be ignored since the phase modulation of the observed image is not observable on the camera. In order to obtain the Fraunhofer diffraction pattern, the second Q operator is then set to be unity, which means (6), shown at the bottom of the page. From (6), the image location of the first-order diffraction is related to $\mathrm{p_{ls}}$, $\mathrm{p_F}$, and $\mathrm{d_1}$. This also means we are able to fix the image location of first-order diffraction by adjusting $\mathrm{p_{ls}}$. We assume that $\mathrm{d_4}$ is a constant, $\mathrm{c_2}$. To fix both of the image locations of the zeroth-order diffraction and the first-order diffraction, $\mathrm{p_F}$ and $\mathrm{p_{ls}}$ have to follow the relation in (7) (shown at the bottom of the page) according to (2), (3), and (6). From (7) and (3), we can always find the corresponding $\mathrm{p_{ls}}$ and $\mathrm{d_1}$ when $\mathrm{p_F}$ changes. $\mathrm{p_{ls}}$ and $\mathrm{d_1}$ (because $\mathrm{d_1}$ is a function of $\mathrm{p_{l1}}$) are controllable by two liquid lenses. This also means we can adjust the focal length of the two liquid lenses in order to keep the image location of the zeroth-order diffraction and the first-order diffraction constant.

Since we have fixed the image location of the zeroth-order diffraction and the first-order diffraction, the magnification can also be derived. After ignoring the first Q operator in (4) and setting the second Q operator to be unity, the transform operator T can be expressed as

$$T = V[\frac{1}{\lambda(d_2 + d_4 - d_2 \cdot d_4 \cdot p_{ls}(A,\lambda)}] \cdot Ff. \qquad (8)$$

Then, the magnification of the output image M can be written as (9), shown at the bottom of the page. After putting $\mathrm{d_3} = \mathrm{c_1}$ and $\mathrm{d_4} = \mathrm{c_2}$ into (9), M is

$$\mathrm{M}(\lambda, p_{ls}(A,\lambda)) = \lambda \times (d_2 + c_2 - d_2 \cdot c_2 \cdot p_{ls}(A,\lambda)). \qquad (10)$$

From (10), we can see that the projected image size can be magnified by manipulating the lens power $p_{ls}(A,\lambda)$ which depends on the applied electric current. As a result, the mismatch of chromatic images can be adjusted electrically by liquid lenses. In addition, the corresponding $\mathrm{d_1}$ and $\mathrm{p_F}$ can be obtained from (3) and (7). $\mathrm{d_1}$ is determined by $\mathrm{p_{l1}}$ which is electrically controllable from (1). Therefore, we can design the holographic projection system using two liquid lenses. The system exhibits not only an electrically tunable optical zoom, but also fixed image locations of the zeroth-order diffraction and first-order diffraction.

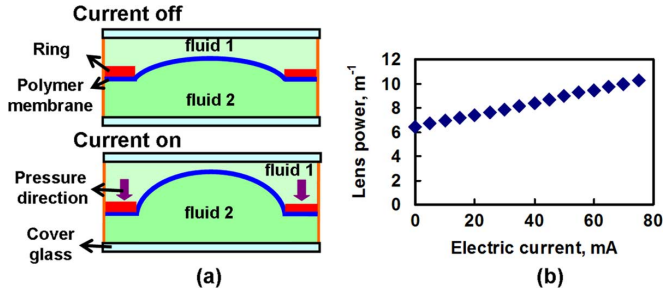

Fig. 2. (a) Working principle of liquid lenses. (b) Measured lens power as a function of the electrical current through a liquid lens. λ : 632.8 nm.

III. Experimental Results and Discussions

To demonstrate the concept of a holographic projector with electrically tunable optical zoom, we adopt the reflective LCoS panel (LC-R 2500, HOLOEYE) and two liquid lenses: "liquid lens 1"(ML-20-35-VIS-LD, Optotune) with an aperture size of 20 mm and "liquid lens 2"(EL-10-30-VIS-LD, Optotune) with an aperture size of 10 mm. The resolution of the LCoS panel is 1024×768 with a pixel pitch of 19 μm. The working principles of the electrically tunable liquid lens ("liquid lens 2") are shown in Fig. 2(a). The liquid lens consists of glass substrates, two optical fluids and a polymer membrane as a separator. The polymer membrane, a special selection of polymers, offers good optical and mechanical properties, such as high elasticity, a large elongation at break, low haze, are transmissive >90% from 240 to 2200 nm, non-absorbing (damage thresholds >25 kW/cm ^{2}), long-term stable and easy to process [12]. When an electric current is applied to the liquid lens, a piezoelectric ring transducer pushes the polymer membrane in the outer part of the lens and then the "fluid 2" is pumped to the center of the lens. The curvature of the polymer membrane is changed. As a result, the lens power of the liquid lens changes. When the liquid lens is used in the holographic projection system, the liquid lens does not need to change the position to affect the zooming properties of the system, only change the lens power at the same position. The measured lens power of the liquid lens as a function of electrical current is shown in Fig. 2. The measured lens power of the liquid lens ("liquid lens 2") can be switched from 6.44 $\mathrm{m^{-1}}$ to 10.27 $\mathrm{m^{-1}}$ when the applied electrical current increases from 0 to 75 mA. The curvature of "liquid lens 1" is mechanically tunable. The measured lens power of the liquid lens ("liquid

$$d_4(p_{ls}(A,\lambda), p_F(\lambda), d_1(p_{l1}(\lambda))) = \frac{d_1(p_{l1}(\lambda)) + d_2 - d_1(p_{l1}(\lambda)) \cdot d_2 \cdot p_F(\lambda)}{p_{ls}(A,\lambda) \cdot (d_1(p_{l1}(\lambda)) + d_2 - d_1(p_{l1}(\lambda)) \cdot d_2 \cdot p_F(\lambda)) - (1 - d_1 \cdot p_F(\lambda))}. \qquad (6)$$

$$p_{\mathrm{F}}(\lambda) = \frac{c_1 - c_2}{(c_1 \cdot d_2 \cdot p_{ls}(A,\lambda) - c_1 - d_2) \cdot (c_2 \cdot d_2 \cdot p_{ls}(A,\lambda) - c_2 - d_2)}. \qquad (7)$$

$$\mathrm{M}(\lambda, p_{ls}(A,\lambda), p_F(\lambda, \mathrm{d_1}) = \lambda \times (d_2 + d_4(p_{ls}(A,\lambda), p_F(\lambda), d_1) - d_2 \cdot d_4(p_{ls}(A,\lambda), p_F(\lambda), d_1) \cdot p_{ls}(A,\lambda)) \qquad (9)$$

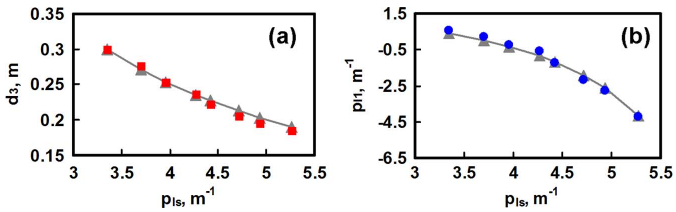

Fig. 3. (a)d_3 as a function of p_{ls} when $p_{l1} = 0.56$ m^{-1}. Red squares stand for experimental results and gray triangles stand for theoretical prediction. (b) p_{l1} as a function of p_{ls} when $d_3 = 0.3$ m. Blue dots stand for experimental results and gray triangles stand for theoretical prediction.

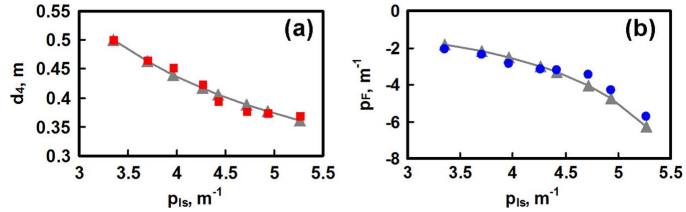

Fig. 4. (a) d_4 as a function of p_{ls}. $p_F = -2.07$ m^{-1}. Red squares represent experimental results and gray triangles represent theoretical prediction. (b) p_F as a function of p_{ls}. $d_4 = 0.5$ m. Blue dots squares represent experimental results and gray triangles represent theoretical prediction.

lens 2") can be switched from -16.5 m^{-1} to 20.2 m^{-1} when we pressed the ring manually. Actually, the "liquid lens 1" can also use the electrically tunable one. The resolution of the liquid lens we measured is 15 lp/mm for modulation transfer function (MTF) >0.5. The response times of the liquid lens from 0 mA to 75 mA and 75 mA to 0 mA for light intensity at focus switched between 10% and 90% and between 90% and 10% are $\sim$ 35 ms and $\sim$ 78 ms. The slow response time may be because it takes time to change the volume of the liquid as we switch the piezoelectric transducer. The power consumption of the liquid lens is in a range between 30.4 mW and 92.4 mW when the driving voltage is switched from 0.76 V (current: 40 mA) to 1.32 V (current: 70 mA).

To measure d_3 as a function of p_{ls}, we then arranged the experimental setup as shown in Fig. 1(a). In experiments, L was 2.37 m, d_0 was 10 cm, d_2 was 20 cm, and the lens power of the solid lens was -5 m^{-1}. c_1 was set at 30 cm. A current of 40 mA was applied to "liquid lens 2" and then we adjusted the lens power of the "liquid lens 1" ($\sim$ 0.56 m^{-1}) in order to make sure the light focused at $d_3 = 30$ cm after light passed through the solid lens. The lens power of the "liquid lens 1" was then set as $\sim$ 0.56 m^{-1}. Then we increased the current of the "liquid lens 2" from 40 mA to 75 mA which meant the corresponding lens power of p_{ls} was increased from 3.35 m^{-1} to 5.27 m^{-1}. Then we measured the distance d_3 which is the distance between the solid lens and the focal spot of the zeroth-order diffraction. The measured results are shown in red squares in Fig. 3(a). In Fig. 3(a), d_3 decreases from 30 cm to 18.5 cm when p_{ls} increases from 3.35 m^{-1} to 5.27 m^{-1}. The gray triangles in Fig. 3(a) stand for the theoretical prediction based on (2) which agrees well with the experiments. As a result, when the lens power of "liquid lens 1" is fixed (i.e., p_{l1} is fixed), the image location of zeroth-order diffraction (i.e., d_3) changes with the lens power of "liquid lens 2"(i.e., p_{l2}). That also means the high pass filter has to be moved around to block out the zeroth-order diffraction when the power of "liquid lens 2" is adjusted for changing the image size at different wavelengths. In order to keep d_3 a constant, the lens power of the "liquid lens 1"(i.e., p_{l1}) should be adjusted when p_{ls} changes. To find out the relation between p_{l1} and p_{ls}, we put the screen 30 cm in the rear of the solid lens (i.e., $d_3 = 30$ cm) and observed the spot size on the screen. When the electric current of "liquid lens 2" was increased, we observed an enlarged laser spot on the screen. Therefore, we compensated this by adjusting the electric current of "liquid lens 1"(p_{l1}) in order to reduce the laser spot size and thereby maintain the minimum laser spot size on the screen. We then recorded p_{l1} and the current from which p_{ls} can be calculated. p_{l1} as a function of p_{ls} is shown in Fig. 3(b) (blue dots) which agrees well the theoretical prediction of (1) (gray triangles). As a result, we can always find out a corresponding p_{l1} as p_{ls} changes in order to maintain the position of zeroth-order diffraction.

To measure the image location of first-order diffraction (d_4) as a function of p_{ls}, we input a Fourier hologram with the resolution 384×384 pixels. From previous paragraph, p_{l1} was 0.56 m^{-1} and $d_3 = 30$ cm. We placed the screen at 50 cm away from the solid lens. (i.e., $d_4 = 50$ cm) and we recorded images on the screen using a webcam (Logitech, PR9000). We then adjusted the lens power of the Fresnel lens (p_F) and analyzed the corresponding images. When p_F equals to -2.09 m^{-1}, the contrast ratio of the image is maximum. The value of p_F was then fixed at -2.09 m^{-1}. We then increased p_{ls} by changing the current of the "liquid lens 2" and also changed p_{l1} according to Fig. 3(b) in order to keep $d_3 = 30$ cm. We moved the screen to record the images and recorded the distance (d_4) between the screen and the solid lens when the contrast ratio of the image is maximal. d_4 as a function of p_{ls} is shown in Fig. 4(a). d_4 decreases from 50 cm to 36.9 cm when p_{ls} increases from 3.35 m^{-1} to 5.27 m^{-1}. The experimental results agree well with the theoretical prediction of (6). This indicates that when p_F is unchanged, the image location of first-order diffraction (d_4) changes with the lens power of the "liquid lens 2" (p_{ls}) even though the image location of zeroth-order diffraction (d_3) is unchanged.

Next, we measure p_{ls} as a function of p_F when d_4 is fixed ($d_4 = 50$ cm). Once again, we increased p_{ls} by changing the current of the "liquid lens 2" and also changed p_{l1} according to Fig. 3(b) in order to keep $d_3 = 30$ cm. We then changed p_F and recorded the images on a screen using a webcam. When the contrast ratio of the image is maximal, we recorded the value of p_F. p_{ls} as a function of p_F is shown in Fig. 4(b). p_F decreases from -2.09 m^{-1} to -5.7 m^{-1} when p_{ls} increases from 3.35 m^{-1} to 5.27 m^{-1}. The experimental results agree well with the theoretical prediction of (7). As a result, when we adjust the lens power of the Fresnel lens (p_F), we can always find a corresponding lens power p_{ls} by adjusting the current of the "liquid lens 2" in order to keep both image locations of zeroth-order diffraction and first-order diffraction (d_3 and d_4) unchanged.

To measure the magnification, we input a Fourier hologram with the resolution 384×384 pixels and projected at the screen 50 cm in the rear of the solid lens. In the experiments, the distances of d_2, d_3 and d_4 in Fig. 1(c) were set at 20 cm, 30 cm, and 50 cm, respectively. We did similar experiments to change

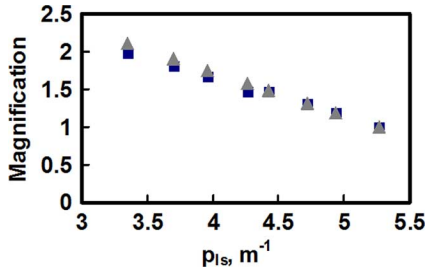

Fig. 5. The magnification as a function of p_{ls}. Blue squares stand for the experimental results and gray triangles stand for theoretical prediction.

p_{l1}, and p_F as p_{ls} changes in order to obtain fixed image locations of the zeroth-order diffraction and the first-order diffraction ($d_3 = 30$ cm and $d_4 = 50$ cm). A webcam was used to take photos of the screen and calculate the magnification by comparing the sizes of images. For calibration, the image when $p_{ls} = 5.27\ m^{-1}$ (i.e., A = 75 mA), $p_{l1} = -4.19\ m^{-1}$, $p_F = -5.7\ m^{-1}$ was set as M = 1. Fig. 5 shows the magnification as a function of p_{ls} (blue squares). The magnification decreases from 1.98 to 1 when p_{ls} increases from 3.35 m^{-1} to 5.27 m^{-1}, p_{l1} increases from $-4.19\ m^{-1}$ to 0.56 m^{-1}, and p_F increases from $-5.7\ m^{-1}$ to $-2.09\ m^{-1}$. The theoretical prediction (gray triangles) is similar to the experimental results. The zoom ratio is 1.98:1 in Fig. 5. Therefore, by adjusting the lens powers of "liquid lens 1", "liquid lens 2" and the encoded Fresnel lens, we can change the size of the projected image while maintaining the image locations of zeroth-order diffraction and the first-order diffraction.

To compare the images with and without the zeroth-order diffraction, we captured the images on the screen without and with the optical high pass filter, as shown in Figs. 6(a) and (b). The parameters of the experimental setup are: L = 2.37 m, $d_0 = 10$ cm, $d_2 = 20$ cm, $d_3 = 30$ cm, $d_4 = 50$ cm, a current of 40 mA for "liquid lens 2", $p_{ls} = 3.35\ m^{-1}$, $p_{l1} = 0.56\ m^{-1}$, and $p_F = -2.09\ m^{-1}$. Without the high pass filter, the zeroth-order diffraction seriously affects the image on the screen, as shown in Fig. 6(a). Using a high pass filter to block the zeroth-order diffraction is necessary for a holographic projection system, as shown in Fig. 6(b). In Fig. 6(c), the image is smaller when the wavelength decreases compared to Fig. 6(b). The image size of Fig. 6(b) is 1.20× larger than that of Fig. 6(c). According to (10), the ratio of two wavelengths is $632.8 : 532 = 1.19 : 1$ which is close to 1.20:1. We adjust the lens powers: $p_{ls} = 3.96\ m^{-1}$, $p_{l1} = -0.23\ m^{-1}$, $p_F = -2.86\ m^{-1}$ and the size of the red image in Fig. 6(b) can be reduced to the size of the green image in Fig. 6(c), as shown in Fig. 6(d). Since the location of the zeroth-order diffraction and first-order diffraction are fixed, we can adjust the image size at different wavelengths without changing the high pass filter and the observation plane (screen). Besides, the liquid lenses we used are affected by gravity. Gravity results in an asymmetrical parabolic phase profile of the liquid lens which produces aberration. As a result, the image of the first-order diffraction is distorted and this affects the image quality of the projected image. However, the aberration of the liquid lens can be compensated by adjusting the hologram on the LCoS device. The image quality can also be improved by improving the liquid lenses or liquid crystal lenses

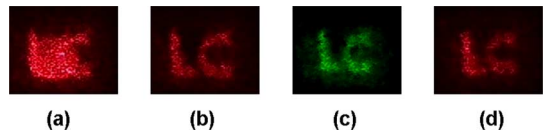

Fig. 6. Projected images of "LC": (a) without a high pass filter (λ : 632.8 nm, the current of the "liquid lens 2" 40 mA); (b) with a high pass filter (λ : 632.8 nm, the current of the "liquid lens 2"=40 mA), and (c)with a high pass filter λ : 532 nm, the current of the "liquid lens 2"=40 mA). In (a), (b), (c), $p_{ls} = 3.35\ m^{-1}$, $p_{l1} = 0.56\ m^{-1}$, $p_F = -2.09\ m^{-1}$. (d) The projected image with a high pass filter (λ : 632.8 nm, the current of the "liquid lens 2" =50 mA, $p_{ls} = 3.96\ m^{-1}$, $p_{l1} = -0.23\ m^{-1}$, $p_F = -2.56\ m^{-1}$).

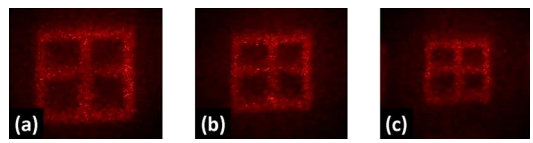

Fig. 7. Projected images of "田" with a high pass filter. (a) The current of the "liquid lens 2"=40 mA, $p_{ls} = 3.35\ m^{-1}$, $p_{l1} = 0.56\ m^{-1}$, $p_F = -2.09\ m^{-1}$. and (b) the current of the "liquid lens 2"=50 mA, $p_{ls} = 3.96\ m^{-1}$, $p_{l1} = -0.23\ m^{-1}$, $p_F = -2.86\ m^{-1}$, and (c) the current of the "liquid lens 2"=60 mA, $p_{ls} = 4.42\ m^{-1}$, $p_{l1} = -1.24\ m^{-1}$, $p_F = -3.2\ m^{-1}$. $\lambda = 632.8$ nm.

[13]–[15]. The image quality of tunable focusing liquid lenses has been reported [16]–[19]. In order to achieve a fast refresh rate, the response time of the liquid lenses should be faster. A tunable focusing lens using blue phase liquid crystals can be fast <1 ms [20]. This should be fast enough for the color-sequential approach.

The image size can also be changed by changing the lens power of the liquid lens. In Fig. 7, we projected a lattice pattern and changed the current of "liquid lens 2". The image size reduces when p_{ls} increases, p_{1l} decreases and p_F decreases. Therefore, the image size of the first-order diffraction is tunable by adjusting the lens powers of the liquid lenses while keeping the zeroth-order diffraction blocked.

IV. Conclusion

We have demonstrated an electrically tunable optical zooming holographic projection system with a fixed location of zeroth-order diffraction. By adding two liquid lenses in a holographic projection system, we can fix the locations of both of the zeroth-order and the first-order diffraction and change the size of the projected image at the same time. Therefore, we can remove the zeroth-order diffraction by using a fixed optical high-pass filter. The zoom ratio of our system is $\sim 1.98 : 1$ which is large enough to compensate the mismatched image size in the visible range (i.e., 700:400 or 1.75:1). When the image quality of the liquid lens is good enough, the focusing spot of zeroth-order diffraction is small and we can block this spot by using a small spatial filter. In this way, we can filter away the zeroth-order diffraction without affecting first-order diffraction. The best way to improve the image quality is to improve the performance of the liquid lens. We demonstrate the concept using two wavelengths in this paper. The required optical zoom ratio is 1.75:1 in visible range (400–700 nm), but the optical zoom ratio in the experiments can be up to 1.98:1 for red light. As a result, our design can be used to realize full color projected imaging. The optical zoom function enhances the

feasibility to realize a high resolution, three color, holographic projection system.

ACKNOWLEDGMENT

The authors would like to thank Prof. S.-H. Lin (NCTU), Dr. C.-H. Lin (NCTU), and E. Liao and S. Hong (Jasper Display Corporation) for technical assistance and support.

REFERENCES

[1] A. Georgiou, J. Christmas, J. Moore, A. J. Chapman, A. Davey, N. Collings, and W. A. Crossland, "Liquid crystal over silicon device characteristics for holographic projection of high-definition television images," *Appl. Opt.*, vol. 47, pp. 4793–4803, 2008.

[2] E. Buckley, "Holographic laser projection," *J. Display Technol.*, vol. 7, no. 3, pp. 135–140, Mar. 2011.

[3] E. Buckley, "(2010). Holographic projector using one lens," *Opt. Lett.*, vol. 35, pp. 3399–3401, 2010.

[4] D. Teng, L. Liu, Z. Wang, B. Sun, and B. Wang, "All-around holographic three-dimensional light field display," *Opt. Commun.*, vol. 285, pp. 4235–4240, 2012.

[5] M. Makowski, I. Ducin, K. Kakarenko, A. Kolodziejczyk, A. Siemion, J. Suszek, M. Sypek, and D. Wojnowski, "Efficient image projection by Fourier electroholography," *Opt. Lett.*, vol. 36, pp. 3018–3020, 2011.

[6] M. Makowski, M. Sypek, I. Ducin, A. Fajst, A. Siemion, J. Suszek, and A. Kolodziejczyk, "Experimental evaluation of a full-color compact lensless holographic display," *Opt. Express*, vol. 17, pp. 20840–20846, 2009.

[7] B. Marx, "Holographic optics-miniature laser projector could open new markets," *Laser Focus World*, vol. 42, p. 40, 2006.

[8] H. C. Lin, N. Collings, M. S. Chen, and Y. H. Lin, "A holographic projection system with an electrically tuning and continuously adjustable optical zoom," *Opt. Exp.*, vol. 20, pp. 27222–27229, 2012.

[9] M. Makowski, I. Ducin, K. Kakarenko, J. Suszek, M. Sypek, and A. Kolodziejczyk, "Simple holographic projection in color," *Opt. Express*, vol. 20, pp. 25130–25136, 2012.

[10] M. Nazarathy and J. Shamir, "Fourier optics described by operator algebra.," *J. Opt. Soc. Amer.*, vol. 70, pp. 150–159, 1980.

[11] J. W. Goodman, *Introduction to Fourier Optics*, 2nd ed. New York, NY, USA: McGraw-Hill, 1996.

[12] M. Blum, M. Büeler, C. Grätzel, and M. Aschwanden, "Compact optical design solutions using focus tunable lenses.," in *Proc. SPIE*, 2011, vol. 8167, p. 81670W.

[13] S. Xu, H. Ren, and S. T. Wu, "Dielectrophoretically tunable optofluidic devices," *J. Phys. D: Appl. Phys.*, vol. 46, p. 483001, 2013.

[14] L. Ren, S. Park, H. Ren, and I. Yoo, "Adaptive liquid lens by changing aperture," *J. Microelectromech. Syst.*, vol. 21, p. 953, 2012.

[15] H. Ren and S. T. Wu, *Introduction to Adaptive Lenses*, 1st ed. Hoboken, NJ, USA: Wiley, 2012.

[16] H. C. Lin and Y. H. Lin, "An electrically tunable focusing pico-projector adopting a liquid crystal lens," *Jpn. J. Appl. Phys.*, vol. 49, 2010, Art. ID 102502.

[17] J. Y. Yiu, R. Batchko, S. Robinson, and A. Szilagyi, "A fluidic lens with reduced optical aberration," in *Proc. SPIE*, 2012, vol. 8301, p. 830117.

[18] J. H. Sun, B. R. Hsueh, Y. C. Fan, J. MacDonald, and C. C. Hu, "Optical design and multiobjective optimization of miniature zoom optics with liquid lens element," *Appl. Opt.*, vol. 48, pp. 1741–1757, 2009.

[19] S. Murali, P. Meemon, K. S. Lee, W. P. Kuhn, K. P. Thompson, and J. P. Rolland, "Assessment of a liquid lens enabled *in vivo* optical coherence microscope," *Appl. Opt.*, vol. 49, pp. D145–D156, 2010.

[20] Y. H. Lin, H. S. Chen, H. C. Lin, Y. S. Tsou, H. K. Hsu, and W. Y. Li, "Polarizer-free and fast response microlens arrays using polymer-stabilized blue phase liquid crystals," *Appl. Phys. Lett.*, vol. 96, Art. ID 113505.

Ming-Syuan Chen received the B.S. degree in electrical engineering and computer science form National Chiao Tung University, Hsinchu, Taiwan, in 2010, and is currently working toward the Ph.D. degree at Department of Photonics, National Chiao University, Hsinchu, Taiwan.

His current research interests include the development of phase modulators, liquid crystal lenses and the designs of electrically tunable optical zoom systems based on liquid crystal lenses.

Neil Collings was born in Stalybridge, Cheshire in 1949. He was educated at Manchester Grammar School, and received the B.A.(Hons.) degree in natural sciences from Trinity Hall, Cambridge University, Cambridge, U.K., in 1971, and the Ph.D. degree in physics from the University of Salford in 1977.

At the beginning of his career, he worked in birefringence studies and optical sensors. He began studying liquid crystal spatial light modulators and their application to optical correlators during his work at the Standard Telecommunications Laboratories between 1984 and 1989. He wrote a book entitled "*Optical Pattern Recognition Using Holographic Techniques*" (Addison-Wesley, 1988), based on his research during this period. He continued working in the field of liquid crystal devices and their associated optical systems until he moved to the University of Cambridge in 1999. He is currently a Reader in Liquid Crystal Photonics in the Photonics & Sensors group of the Department of Engineering.

Dr. Collings is a Fellow of the Institute of Physics and a Senior Member of SPIE.

Hung-Chun Lin received the B.S. degree in electrical engineering from National Sun Tat-Sen University (Taiwan), in 2005, the M.S. degree from the Display Institute, National Chiao Tung University (Taiwan), in 2007, and the Ph.D. degree from the Department of Photonics, National Chiao Tung University (Taiwan), in 2012.

His research interests include the liquid crystal and polymer composite film, liquid crystal lenses and the designs of electrically tunable optical systems based on liquid crystal lenses.

Yi-Hsin Lin received the B.S. degree in physics from National Tsing Hua University (Taiwan), in 1998, the M.S. degree from the Institute of Electro-Optical Engineering, National Chiao Tung University (NCTU, Taiwan), in 2000, and the Ph.D. degree in optics from the College of Optics and Photonics: CREOL & FPCE, University of Central Florida, Orlando, FL, USA, in 2006.

She is currently an associate professor in the Department of Photonics of NCTU (Taiwan). Several papers were selected as cover pages or feature articles in *Physical Review Letters* and *Optics Express*. The research interests of Prof. Lin are in physics of liquid crystals (LC), LC-based optical devices, and bio-sensing based on a liquid crystal/polymer system.

Prof. Lin is a recipient of Glenn H. Brown Prize awarded by International Liquid Crystal Society (ILCS) in 2008, the 2006 OSA New Focus/Bookham award, 2005 Newport Research Excellence award, and several other awards.